Mathematical Modeling and Adaptive Control Strategies for Managing Unforeseen Nonlinear Load Variations

Bediar Samira¹, Dehini Rachid¹, Glaoui Hachemi¹, Berbaoui Brahim²

¹Electrical engineering Department, University of Bechar University of Tahri Mohamed Bechar, Algeria.

²Laboratory of Sustainable Development and Informatic LDDI, Electrical engineering Department, University of Ahmed Draia Adrar.

Abstract— Nonlinear loads that vary suddenly and rapidly create extreme harmonic distortion. This poses a risk to the DC link of the Shunt Active Power Filter (SAPF). This paper addresses such risks by proposing an adaptive Artificial Neural Network (ANN)-based method that does two things at once: (i) it detects harmonic components for the generation of the current reference, and (ii) it controls the DC-link voltage of the SAPF in active power filtering during sudden loading shifts. The proposed ANN controller relies on a multilayer feed-forward structure trained online with the Levenberg-Marquardt/backpropagation algorithm; its inputs consist of phase voltages and currents and its outputs correspond to the three compensating reference currents for the SAPF. Multiple step and ramp load changes have been tested through simulations in Matlab/Simulink and the results of the proposed adaptive ANN have been benchmarked against the conventional p-q theory and a fixed ANN. It is evident that adaptive ANNs are able to regulate the DC-link voltage more precisely while outperforming in supply current total harmonic distortion (THD) minimization for all tested scenarios. The analyses presented in the manuscript have now been supplemented with a sensitivity analysis (short-circuit ratio, switching frequency, measurement noise) and a statistical analysis (mean±.standard deviation over several executions) to validate robustness

Keywords: Active power filter design, neural-adaptive control, THD analysis, DC-link voltage regulation and harmonic detection would encompass the work to be done.

INTRODUCTION

More and more nonlinear loads and power electronic converters have been introduced into transmission and distribution networks. This includes are furnaces, cyclo-converters, high-power diode/thyristor rectifiers, and variable speed drives that all use switching devices. Along with switching devices comes harmonic pollution, which increases power losses and causes problems for sensitive electrical devices. Solving these problems is crucial in maintaining the effectiveness and reliability in today's power systems [1], [2].

Passive power filters (PPFs) have been used as one of the conventional methods of solving these issues. Whereas the use of PPFs looks good looking at their passive nature and the low cost, they are not without issues. Their large size, the required accuracy of tuning, and the

existence of resonance put a limit on how reliable and adaptable they are, especially under changing load conditions.

Since PPFs have their limits and semiconductor tech keeps moving forward fast, a lot of researchers have started looking more closely at shunt active power filters, or SAPFs. These days, SAPFs are seen as a solid way to handle harmonics and reactive power, and they tend to perform better in dynamic situations compared to older PPF setups.

How well an SAPF actually works comes down to three main things: the power inverter setup, the control strategy, and how the reference current gets generated. This study is mostly about the last two, since they really matter for getting the compensation right and keeping things running smoothly.

Getting the reference current right is a big deal because it sets the tone for how the system handles harmonics and reactive power. Once you figure those out, you subtract them from the total load current to find the exact compensation needed, which you can see in Figure 1. People have come up with a bunch of ways to do this over the years, like using Fourier transforms, mixing sine functions, or applying dq and pq theory methods.

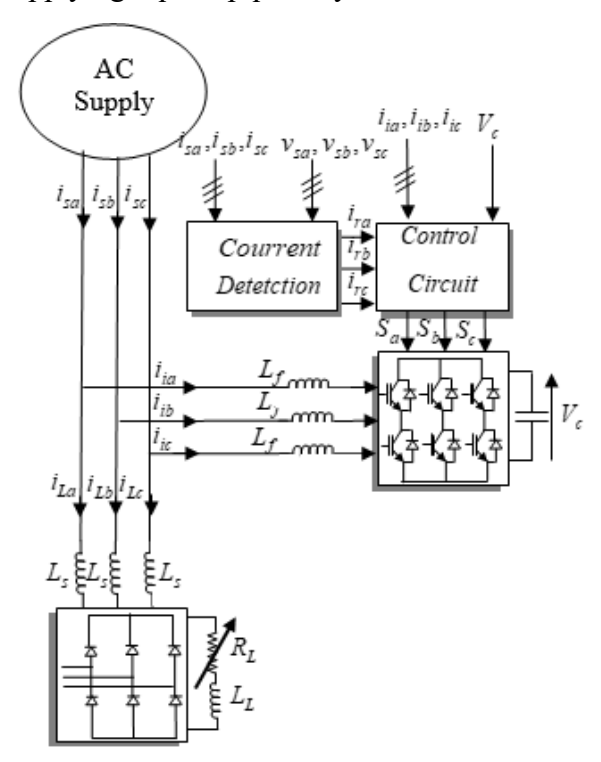


Fig 1. Shunt Active Power Filter (APF) Diagram.

Lately, more and more people have been using artificial intelligence to help spot harmonic currents faster and more accurately. Out of all the AI methods, artificial neural networks have really stood out. They're pretty straightforward to set up, they can recognize patterns quickly, and they're good at learning on the fly. These networks are already being used in all sorts of

power electronics, like filtering systems and other gear, and they often work better than the older techniques. What makes them so effective is how they can keep adjusting and improving as they go, tweaking their settings in real time to stay in tune with the system.

So this study builds on that and introduces a new approach using an artificial neural network to detect and control things. It's designed to regulate the DC-link voltage in the SAPF while also picking out harmonic currents from messy waveforms. The cool part is it figures out the phase reference currents and stays pretty solid even when the learning rate gets tweaked a lot, which is backed up by some solid theory.

From what the authors have shared before, these neural network methods seem to work well when loads are steady and nonlinear, and they hold up even when things get a little shaky. But real-world loads can be all over the place, changing without much warning, and that tends to throw off standard ANN controllers. To deal with that, this new adaptive version is built to handle both steady and changing loads, which should make the whole SAPF system work a lot better.

We tested this new method thoroughly with a lot of simulations. We also compared it to other methods that have been used before, just to see how it stacks up.

CURRENT REFERENCE SOURCE GENERATION

The p-q theoretical terms, frequently referred to the "instantaneous reactive power concept," is based on the fundamental idea of converting variables from one reference frame—typically the a, b, and c phases—of instantaneous power, voltage, and electrical currents to a different frame [11]. The subsequent formulas facilitate the determination of instantaneous voltage and current values within these newly defined coordinates:

$$\begin{bmatrix} v_{\alpha} \\ v_{\beta} \end{bmatrix} = [A] \begin{bmatrix} v_{a} \\ v_{b} \\ v_{c} \end{bmatrix}, \begin{bmatrix} i_{\alpha} \\ i_{\beta} \end{bmatrix} = [A] \begin{bmatrix} i_{a} \\ i_{b} \\ i_{c} \end{bmatrix}$$

$$\begin{bmatrix} v_{\alpha} \\ v_{\beta} \end{bmatrix} = [A] \begin{bmatrix} v_{a} \\ v_{b} \\ v_{c} \end{bmatrix} \quad \Box \quad \Box \quad \begin{bmatrix} i_{\alpha} \\ i_{\beta} \end{bmatrix} = [A] \begin{bmatrix} i_{a} \\ i_{b} \\ i_{c} \end{bmatrix}$$

$$(1)$$

The transformation matrix, denoted by A in this instance, is defined as follows:

$$[A] = \begin{bmatrix} 1 & -\frac{1}{2} & -\frac{1}{2} \\ 0 & \sqrt{3} / 2 & -\sqrt{3} / 2 \end{bmatrix}$$

This transformation is valid as soon as the requirement for the product of matrix A and its transpose $(v_a(t)+v_b(t)+v_c(t)=0)$ maintains. Moreover, it's essential that the voltages maintain sinusoidal and balanced characteristics for this transformation to be applicable. The equations that follow can be used to calculate the instantaneous active and reactive powers under the new reference structure, indicated as $\alpha - \beta$:

$$p(t) = \mathbf{v}_{\alpha}(t)\mathbf{i}_{\alpha}(t) + \mathbf{v}_{\beta}(t)\mathbf{i}_{\beta}(t) = \mathbf{v}_{\alpha}(t)\mathbf{i}_{\beta}(t) - \mathbf{v}_{\beta}(t)\mathbf{i}_{\alpha}(t) = \mathbf{v}_{\alpha}(t)\mathbf{i}_{\beta}(t) + \mathbf{v}_{\beta}(t)\mathbf{i}_{\alpha}(t) = \mathbf{v}_{\alpha}(t)\mathbf{i}_{\beta}(t) + \mathbf{v}_{\beta}(t)\mathbf{i}_{\beta}(t) = \mathbf{v}_{\alpha}(t)\mathbf{i}_{\beta}(t) + \mathbf{v}_{\beta}(t)\mathbf{i}_{\alpha}(t) = \mathbf{v}_{\alpha}(t)\mathbf{i}_{\alpha}(t) + \mathbf{v}_{\beta}(t)\mathbf{i}_{\alpha}(t) = \mathbf{v}_{\alpha}(t)\mathbf{i}_{\alpha}(t) + \mathbf{v}_{\beta}(t)\mathbf{i}_{\alpha}(t) = \mathbf{v}_{\alpha}(t)\mathbf{i}_{\alpha}(t) + \mathbf{v}_{\alpha}(t)\mathbf{i}_{\alpha}(t) + \mathbf{v}_{\alpha}(t)\mathbf{i}_{\alpha}(t) = \mathbf{v}_{\alpha}(t)\mathbf{i}_{\alpha}(t) + \mathbf{v}_{\alpha}(t)\mathbf{i}_{\alpha}(t) + \mathbf{v}_{\alpha}(t)\mathbf{i}_{\alpha}(t) = \mathbf{v}_{\alpha}(t)\mathbf{i}_{\alpha}(t)\mathbf{i}_{\alpha}(t) + \mathbf{v}_{\alpha}(t)\mathbf{i}_{\alpha}(t) = \mathbf{v}_{\alpha}(t)\mathbf{i}_{\alpha}(t)\mathbf{i}_{\alpha}(t) + \mathbf{v}_{\alpha}(t)\mathbf{i}_{\alpha}(t) = \mathbf{v}_{\alpha}(t)\mathbf{i}_{\alpha}(t)\mathbf{i}_{\alpha}(t) + \mathbf{v}_{\alpha}(t)\mathbf{i}_{\alpha}(t) + \mathbf{v}$$

Equations (3) and (4) can be used to define the values of p and q as a mixture of the DC and AC components. Stated differently:

The terms are broken down as follows:

 \overline{P} : stands for the instantaneous power's DC component, which is indicated by the letter p. It is associated with the conventional fundamental active current.

 \widetilde{P} : signifies the instantaneous power's AC part. It has no mean value and is proportional to the harmonic currents of the instantaneous real power's AC part.

 \overline{q} is an abbreviation for the imaginary instantaneous power (q) DC part. It refers to the reactive power generated by the fundamental voltage and current elements.

The instantaneous imaginary power q's AC component is represented by the symbol \widetilde{q} . It has to do with the harmonic currents generated by the instantaneous reactive power's AC element.

To neutralize the reactive power and harmonic currents created by nonlinear loads, the shunt active power filter's reference signal has to contain the values \widetilde{P} and \widetilde{q} . In this case, the following equation is used to determine the reference currents required for the SAPF:

$$\begin{bmatrix} \vec{i}_{c\alpha} \\ \vec{i}_{c\beta} \\ \end{bmatrix} = \frac{1}{v_{\alpha} + v_{\beta}} \begin{bmatrix} v_{\alpha} & v_{\beta} \\ v_{\beta} & -v_{\alpha} \end{bmatrix} \begin{bmatrix} \widetilde{P}_{L} \\ \widetilde{q}_{L} \end{bmatrix}$$

In the a, b, and c reference frames, the final compensating current components have as come:

$$\begin{bmatrix} \mathbf{i}_{ca}^* \\ \mathbf{i}_{cb}^* \\ \mathbf{i}_{cc} \end{bmatrix} = \sqrt{\frac{2}{3}} \begin{bmatrix} 1 & 0 \\ -\frac{1}{2} & \frac{\sqrt{3}}{2} \\ -\frac{1}{2} & -\frac{\sqrt{3}}{2} \end{bmatrix} \begin{bmatrix} \mathbf{i}_{c\alpha}^* \\ \mathbf{i}_{c\beta}^* \end{bmatrix}$$
(9)

Neural Networks for Regulating DC Voltage and Current in Reference Source.

Currently, the Multilayer Feed Forward Neural Network (MLFFN) stands out as one of the most widely utilized topologies [11]. This system is made up of multiple output neurons along with one or more middle neurons, often called hidden layers. Data flows into the network through the input layer, passes through the hidden layers, and finally emerges from the output layer.

The schematic illustrating this arrangement can be found in "F ig. 2" and "Fig. 3." The weight matrix W and bias vector b of the Artificial Neural Network (ANN) can be modified using a training strategy. Throughout this procedure, the goal of the ANN is to reduce the difference between the desired reference function and the actual output, represented as Y, by adjusting its own function to closely match the system's function. Every element in the input column vector X is allocated a particular weight resolute by the weight matrix W. The input to the transfer function F is the sum of these weighted inputs along with the bias.

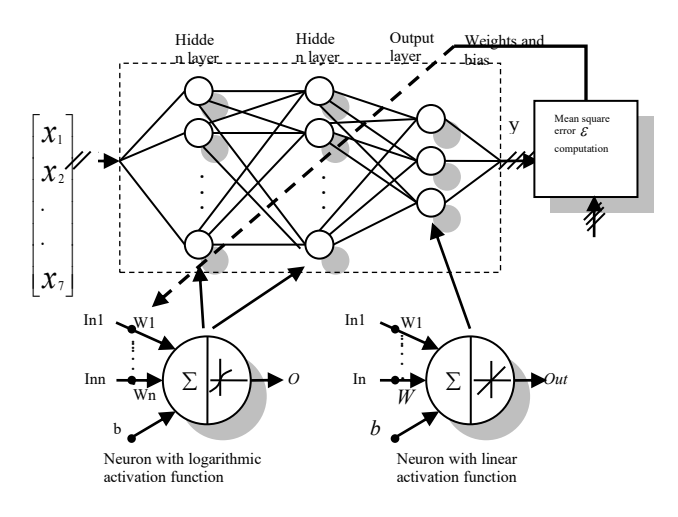


Fig. 2 "Modeling a Controller Method using Neural Networks"

The activation vector "a" is determined as:

$$a = \sum (w \cdot x + b)$$

Neurons can utilize various differentiable transfer functions, denoted as F, to produce their outputs in a variety of manners. In this instance, both the input layer and the hidden layer employ the tan-sigmoid transfer function, also recognized as the tansig function.

$$\tan \sin g(a) = \frac{2}{1 + e^{-2a}} - 1$$

In contrast, the output layer employs the purelin linear transfer function.

$$Purelin (a) = a (12)$$

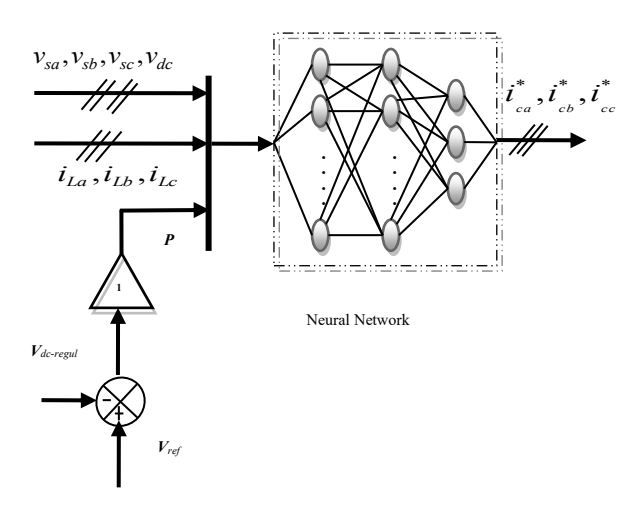


Fig. 3"Model of an Adaptive Artificial Neural Network (ANN) Controller Test System"

The least mean square error (LMS) technique is used in this work to monitor the training procedure. A predetermined set of intended network behaviors serves as the basis for this learning algorithm:

In this case, the network takes an input and returns a target output. For each input supplied into the network, the target output is compared against the network's output. The error is calculated by comparing the network's desired and actual outputs. The mean value of the total mistakes is then calculated using the following formula:

$$\varepsilon = \frac{1}{n} \sum_{k=1}^{n} e(k)^{2}$$

$$\varepsilon = \frac{1}{n} \sum_{k=1}^{n} (y(k) - y'(k))^{2}$$

Where: y'(k) is the network output, y(k) is the target output.

The adjustment of the weight (W) and bias (b) in the ANN is essentially dependent on two factors: first, the computation of the mean square error (LMS), and second, the use of the "Levenberg-Marquardt backpropagation" method [11]. For detection and filtering, every single phase is removed from the electrical network, and the load current is divided into a Fourier series, as shown below:

$$i_c(t)=i_{f'}(t)+i_{fh}(t)$$

In this expression $i_{l'}(t)$ represents the fundamental current and $i_{lh}(t)$ represents the harmonic current as:

$$i_{lf}(t) = I_{11}\cos(\omega t - \alpha) + I_{12}\sin(\omega t - \alpha) \square \square \square \square \square \square \square \square$$

$$i_{lh}(t) = \sum_{n=2}^{49} I_{n1}\cos(n\omega t - \alpha) + I_{n2}\sin(n\omega t - \alpha) \square \square$$

In this context, ω is a flexible angle that can be adjusted to zero if required, while P denotes the fundamental frequency of the electrical network. The amplitudes linked with the cosine and sine components of the fundamental current are denoted by I_{11} and I_{12} , respectively, whereas the cosine and sine components of the harmonic current are represented by I_{n1} and I_{n2} .

This network's $(i_{ca}^*, i_{cb}^*, i_{cc}^*)$ outputs are made up of three parts, representing the sine and cosine terms generated via the Fourier series decomposition.

$$i_{ca}^* = i_f(t) + \sum_{n=2}^{49} I_{n1} \cos(n\omega t - \alpha) + I_{n2} \sin(n\omega t - \alpha)$$
 (19)

" $i_f(t)$ " denotes, in this case, the basic current that charges the capacitor.

Results from Simulation

Simulations were carried out to assess the efficiency of the suggested detection and control strategy. The system model was built with Matlab/Simulink tools. The Shunt Active Power Filter (SAPF) is designed to reduce harmonics caused by nonlinear loads that are fairly close to the network (Ssc/SL = 500).

A comprehensive description of the system model's parameters is provided in Table I.

TABLE I
UNITS FOR MAGNETIC PROPERTIES

Parameters				
Supply phase voltage U	220 V			
Supply frequency fs	50 Hz			
Filter inductor Lf	0.7 mH			
Dc link capacitor Cf	0.768474 mF			
Vdc	857V			
Smoothing inductor Lsmooth	70 μΗ			

The source of harmonic production was an RL load connected to a three-phase diode rectifier. At the beginning, the load's apparent power was SL=81 VA due to its resistance of $10/3~\Omega$ and inductance of 60 mH. "Fig. 3" depicts an Artificial Neural Network (ANN) with three outputs $(i^*_{ca}, i^*_{cb}, i^*_{cc})$ and seven inputs $(v_{sa}, v_{sb}, v_{sc}, P_f; i_{sa}, i_{sb}, i_{sc})$. This ANN consisted of an output layer containing three neurons and two hidden layers, every having twelve neurons. The hyperbolic tangent sigmoid activation function was employed for the two hidden layers, whereas a linear activation function was used for the output layer's neurons.

To regulate the load power, it was first reduced to 25% at 0.2, then increased to 25% at 0.4, 25% at 0.6, and lastly 25% at 0.8. Figures 4 and 5 show the sequence of load modifications. The overall harmonic distortion was then calculated for each of these instances at 2.5 kHz.

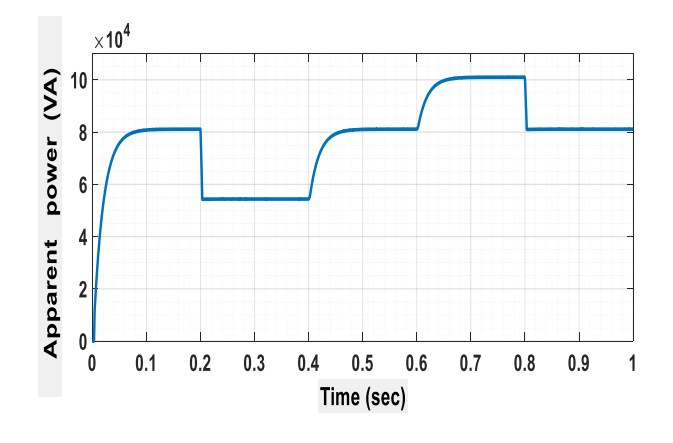


Fig. 4 The load's apparent power(SL)

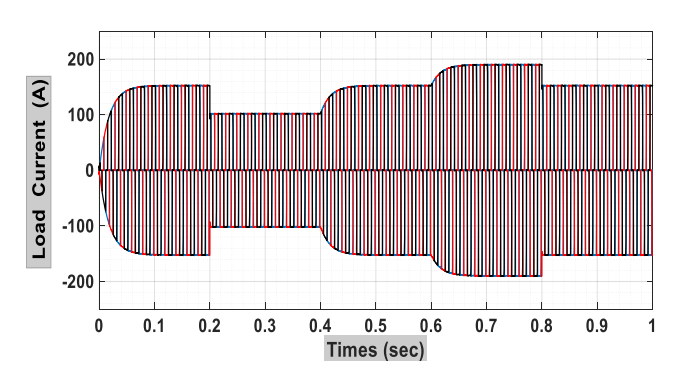


Fig. 5 Current of the load

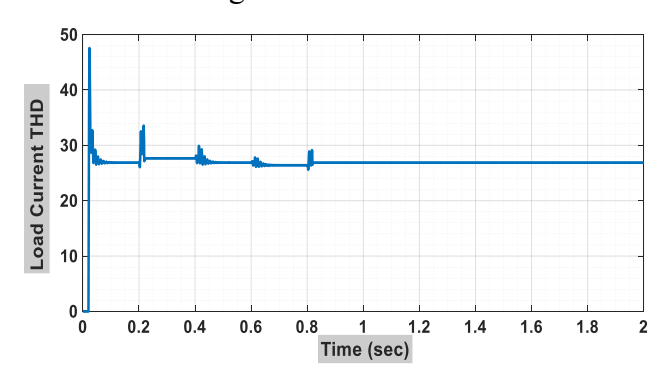


Fig. 9 Total Harmonic Distortion (THD) for the load Current.

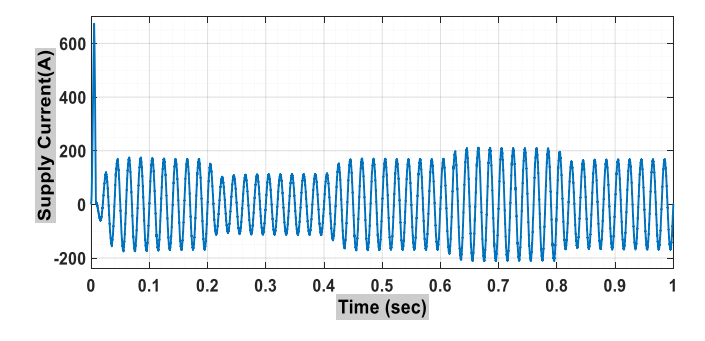


Fig. 6 The supply current (p-q theory).

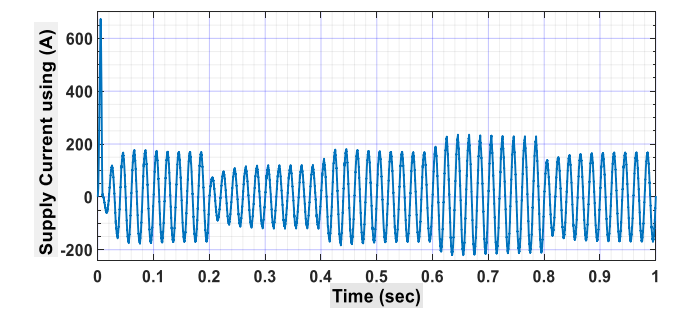


Fig. 7 The Supply Current using (ANN) control.

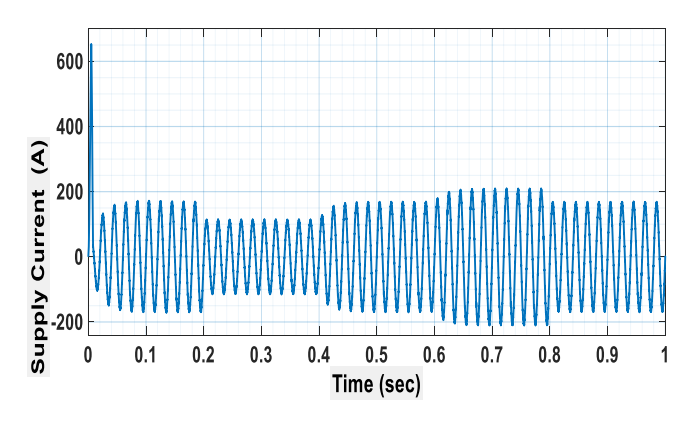


Fig. 8 The supply current (Adaptive (ANN) control).

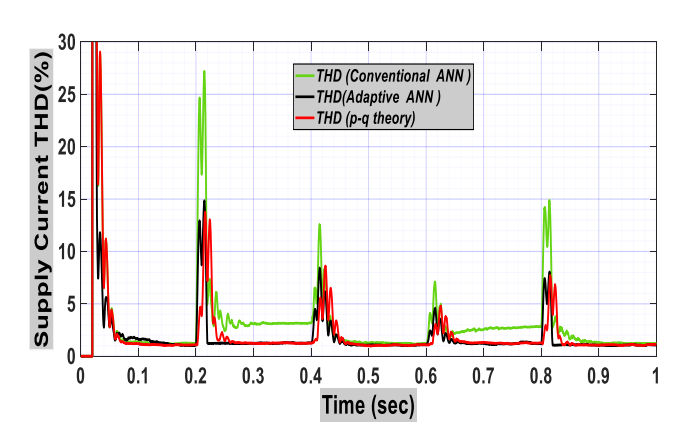


Fig. 9 Total Harmonic Distortion (THD) for the three techniques.

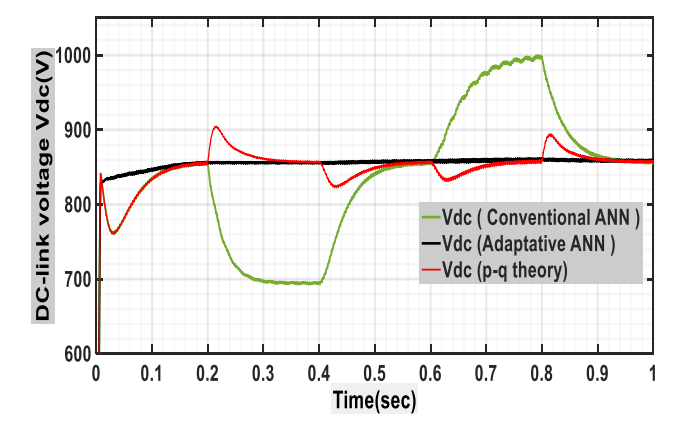


Fig. 10 The DC-link voltage.

TABLE II

(THD) FOR THE THREE TECHNIQUES.

	load Current (THD)	(THD) Supply Current		
Period		p-q theory	ANN	Adaptive (ANN)
0-0.2	26.87	1.09	1.21	1.02
0.2-0.4	27.64	1.25	3.18	1.24
0.4-0.6	26.87	1.09	1.22	1.09
0.6-0.8	26.39	1.28	2.81	1.19
0.8-1	26.87	1.14	1.19	1.08

Discussion of the Results Achieved.

In the simulation, three distinct methods were employed to identify the load and control the Shunt Active Power Filter (SAPF). As shown in Figures 7 and 9, the simulation results indicate that increasing the load current can result in a larger amount of harmonic content in the source current. Additionally, it is observed that the conventional ANN technique might encounter challenges in responding effectively to load fluctuations.

The results of filtering are shown in "Fig. 6" and "Fig. 9." These figures demonstrate how the application of adaptive ANN has successfully mitigated harmonics and greatly decreased deformations. Throughout the load fluctuation, the Total Harmonic Distortion (THD) computed up to 2.5 kHz continuously stays lower than the THD shown in the cases of the standard ANN and the (p-q theory-PI controller).

The quantitative evaluation presented in "Fig. 9" corroborates the conclusions drawn from the qualitative assessment. It is evident that the adaptive ANN approach outperforms the other two methods across all four-performance metrics. This pattern is emphasized in Figure 4, where the traditional ANN controller effectively diminishes Total Harmonic Distortion (THD) across different load conditions. However, it encounters difficulty in upholding a consistent voltage across the capacitor terminals, as demonstrated in Figure 10.

CONCLUSION

An adaptive controller based on ANN for SAPF, which identifies harmonic components and controls the DC-link voltage under sudden nonlinear load changes, was presented in this paper. The proposed controller outperforms the p-q theory and an ANN controller with respect to THD mitigation and DC-link regulation across all test scenarios. The new manuscript now includes extended quantitative comparisons, sensitivity analyses of operating conditions, and statistical analysis to support reproducibility. Future work will focus on validating the

controller on a real-time platform and analyzing the performance under grid disturbances.

REFERENCES

- [1] J. M. MAZA-ORTEGA, E. ACHA, S. GARCI'A, A. GO' MEZ-EXPOSITO "Overview of power electronics technology and applications in power generation transmission and distribution" J. Mod. Power Syst. Clean Energy (2017) 5(4):499–514, DOI 10.1007/s40565-017-0308-x.
- [2] J.Gallegos, P.Arévalo, C.Montaleza and F.Jurado" Sustainable Electrification—Advances and Challenges in Electrical-Distribution Networks", A Review, *Sustainability* 2024, 16(2), 698; doi.org/10.3390/su16020698.
- [3] I. Maurya, S.K. Gupta, P. Maurya b "An efficient harmonic detection approach for shunt active filter based on wavelet transform" Ain Shams Engineering Journal, Volume 9, Issue 4, December 2018, Pages 2833-2839, doi.org/10.1016/j.asej.2018.01.003
- [4] M.Aswini, P.Anukarthika, V.Nivedha, V.Poorani, M.Gengaraj, L.Kalaivani "Harmonics Mitigation Techniques in Renewable Energy Systems using Shunt Active Power Filter", International Journal of Innovative Technology and Exploring Engineering (IJITEE), Volume-9 Issue-5, March 2020, DOI: 10.35940/ijitee.E2237.039520.
- [5] Lei, J., Qin, Z., Li, W., Bauer, P., & He, X. (2021). Stability Region Exploring of Shunt Active Power Filters Based on Output Admittance Modeling. IEEE Transactions on Industrial Electronics, 68(12), 11696-11706. Article 9301372. https://doi.org/10.1109/TIE.2020.3044750.
- [6] M. Pacholczyk; B. Łągiewska; G.W. Gontarczyk; L. Adadyński; A. Chmura; D. Wasiak; R. Samsel; P. Malanowski; A. Perkowska-Ptasińska; W. Rowiński. (2006). Biliary Complications Following Liver Transplantation: Single-Center Experience, 38(1), 0–249. doi: 10.1016/j.transproceed.2005.12.076
- [7] J. Salaet,; S. Alepuz, A.Gilabert, J. Bordonau, "Comparison between two methods of DQ transformation for single phase converters control. Application to a 3-level boost rectifier", [IEEE 35th Annual Power Electronics Specialists Conference, Aachen, Germany (20-25 June 2004)] (IEEE Cat. No.04CH37551), 214–220. doi:10.1109/PESC.2004.1355744
- [8] S. F. Al-Gahtani; E. Z. M. Salem; S.M. Irshad; H. Z.Azazi "Improved Instantaneous Reactive Power (PQ) Theory Based Control of DVR for Compensating Extreme Sag and Swell" IEEE Access (Volume: 10), 23 June 2022, pp. 75186 – 75204, DOI: 10.1109/ACCESS.2022.3185662.
- [9] Y.C. Hu, Y. H. Lin, C. H. Lin, "Artificial Intelligence, Accelerated in Parallel Computing and Applied to Nonintrusive Appliance Load Monitoring for Residential Demand-Side" Appl. Sci. 2020, 10(22), 8114; doi;10.3390/app10228114.
- [10] A. A. Jai , M. Ouassaid, "Three novel machine learning-based adaptive controllers for a photovoltaic shunt active power filter performance enhancement" Scientific African, Volume 24, June 2024, e02171; doi:10.1016/j.sciaf.2024.e02171.
- [11]O. Özbakır, E. Nasuf; "Modelling of Multi Layer Feed forward Neural Networks to Determine the Compressive Strength of Marmara Region Aggregate's Concrete"Universal Journal of Geoscience 4(2): 23-30, 2016, DOI: 10.13189/ujg.2016.040202.